**Molecular Cancer**



# Tetrathiomolybdate inhibits head and neck cancer metastasis by decreasing tumor cell motility, invasiveness and by promoting tumor cell anoikis

*Molecular Cancer* 2010, **9**:206 doi:10.1186/1476-4598-9-206

Pawan Kumar (pawan.kumar@osumc.edu)
Arti Yadav (arti.yadav@osumc.edu)
Samip N Patel (spatel8@health.usf.edu)
Mozaffarul Islam (mozaffarul.islam@osumc.edu)
Quintin Pan (quintin.pan@osumc.edu)
Sofia D Merajver (smerajve@med.umich.edu)
Theodoros N Teknos (ted.teknos@osumc.edu)

**ISSN** 1476-4598

**Article type** Research

**Submission date** 27 May 2010

**Acceptance date** 3 August 2010

**Publication date** 3 August 2010

**Article URL** http://www.molecular-cancer.com/content/9/1/206

# Tetrathiomolybdate inhibits head and neck cancer metastasis by decreasing tumor cell motility, invasiveness and by promoting tumor cell anoikis

Pawan Kumar[1*], Arti Yadav[1], Samip N Patel[2], Mozaffarul Islam[1], Quintin Pan[1], Sofia D Merajver[3], Theodoros N Teknos[1]

[1]Department of Otolaryngology-Head and Neck Surgery and Comprehensive Cancer Center, The Ohio State University, Columbus, OH, USA; [2]Department of Otolaryngology-Head and Neck Surgery, University of South Florida, Tampa, FL, USA; and [3]Department of Internal Medicine, Division of Hematology and Oncology, University of Michigan, Ann Arbor, MI, USA.

**Email addresses:**

PK: pawan.kumar@osumc.edu

AY: arti.yadav@osumc.edu

SNP: spatel8@health.usf.edu

MI: mozaffarul.islam@osumc.edu

QP: quintin.pan@osumc.edu

SDM: smerajve@med.umich.edu

TNT: ted.teknos@osumc.edu

*__Corresponding author:__ Pawan Kumar, Department of Otolaryngology-Head and Neck Surgery, The Ohio State University, 420 W. 12th Avenue, Room # 464, Columbus, OH 43210. Phone: 614-292-2496; E-mail: Pawan.Kumar@osumc.edu.

## ABSTRACT

**Background:** The metastatic spread of solid tumors is directly or indirectly responsible for most cancer-related deaths. Tumor metastasis is very complex and this process requires a tumor cell to acquire enhanced motility, invasiveness and anoikis resistance to successfully establish a tumor at a distal site. Metastatic potential of tumor cells is directly correlated with the expression levels of several angiogenic cytokines. Copper is a mandatory cofactor for the function of many of these angiogenic mediators as well as other proteins that play an important role in tumor cell motility and invasiveness. We have previously shown that tetrathiomolybdate (TM) is a potent chelator of copper and it mediates its anti-tumor effects by suppressing tumor angiogenesis. However, very little is known about the effect of TM on tumor cell function and tumor metastasis. In this study, we explored the mechanisms underlying TM-mediated inhibition of tumor metastasis.

**Results:** We used two *in vivo* models to examine the effects of TM on tumor metastasis. Animals treated with TM showed a significant decrease in lung metastasis in both *in vivo* models as compared to the control group. In addition, tumor cells from the lungs of TM treated animals developed significantly smaller colonies and these colonies had significantly fewer tumor cells. TM treatment significantly decreased tumor cell motility and invasiveness by inhibiting lysyl oxidase (LOX) activity, FAK activation and MMP2 levels. Furthermore, TM treatment significantly enhanced tumor cell anoikis by activating p38 MAPK cell death pathway and by downregulating XIAP survival protein expression.

**Conclusions:** Taken together, these results suggest that TM is a potent suppressor of head and neck tumor metastasis by modulating key regulators of tumor cell motility, invasiveness and anoikis resistance.

## BACKGROUND

Head and neck squamous cell carcinoma (HNSCC) is the sixth most frequent cancer worldwide and five-year survival rates (<50%) are among the lowest of the major cancers [1, 2]. The high mortality associated with advanced head and neck cancers is in large part due to the local spread by primary tumors as well as distal tumor metastasis to vital organs [3, 4]. Pulmonary metastases are the most frequent in HNSCC, accounting for 66% of distal metastases. Other metastatic sites include bone (22%), liver (10%), skin, mediastinum and bone marrow [4]. HNSCC tumors and their vasculature express numerous angiogenic cytokines including vascular endothelial growth factor (VEGF), interleukin (IL) 1α, IL-6, IL-8, and fibroblast growth factor (FGF) [5-7] which facilitate tumor growth and progression. We and others have demonstrated that VEGF expression directly correlates with poor prognosis in head and neck cancer patients [8-11]. We have recently shown that VEGF, in addition to its pro-angiogenic function, also induces the expression of Bcl-2 in the microvascular endothelial cells [12]. Furthermore, tumor samples from head and neck cancer patients showed significantly higher Bcl-2 expression in tumor blood vessels [13] and this enhanced Bcl-2 expression in tumor-associated endothelial cells was directly correlated with metastatic status of these patients [14]. Upregulated Bcl-2 expression in tumor-associated endothelial cells was sufficient to enhance tumor angiogenesis, tumor progression and tumor metastasis of oral squamous cell carcinoma in a SCID mouse model [14].

Tumor metastasis is a complex process consisting of multiple individual steps [15]. The metastatic process requires a tumor cell to acquire the ability to migrate through the primary tumor mass, intravasate and survive in blood or lymphatic vascular system, and extravasate from the vascular system into a secondary organ to form the metastatic nodules. A key process in

basic cell migration is the ability of a cell to form a stable adhesion to the extracellular matrix [16]. This process is regulated by two key proteins within cell: Src and focal adhesion kinase (FAK) [17]. Inactivation of either of these proteins leads to dramatic loss in the cell motility. FAK activation in squamous cell carcinoma and lung adenocarcinoma has been shown to promote cell invasion [18, 19]. In addition, FAK signaling alters matrix metalloproteinases (MMPs, a family of zinc-containing endopeptidases that degrade various components of the extracellular matrix) expression and promotes the generation of an invasive cell phenotype. Overexpression of MMP-2 in tumor tissue has been linked with tumor invasion, metastasis and poor survival in many tumor types including HNSCC [20-22]. FAK gene silencing by RNA interference also inhibited tumor cell metastasis by promoting tumor cell anoikis (anchorage-dependent cells undergoing cell death due to cell detachment) [23]. Recently Payne et al, have demonstrated that lysyl oxidase (LOX), a copper dependent kinase, promotes tumor cell migration and invasiveness via the activation of FAK [24].

Anti-cancer therapy involving copper suppression has been shown to be an effective inhibitor of angiogenesis [25, 26]. Copper is an essential trace element whose distinct angiogenic properties were first discovered in the early 1980's [27]. Copper has since shown to be a direct stimulator of endothelial cell proliferation and migration [27, 28]. Additionally, copper is a required cofactor for the activity, production and secretion of key angiogenic cytokines up-regulated in head and neck cancers [5, 29]. Tetrathiomolybdate (TM) is a potent chelator of copper that has been widely studied for its good oral bioavailability, low toxicity profile and its tumor suppressive effects [25, 30, 31]. We have previously shown that TM is a potent angiogenesis inhibitor and inhibits tumor growth and tumor metastasis [5, 29]. However, the molecular mechanisms by which TM inhibits tumor metastasis are poorly understood. In this

study, we have examined the role and mechanisms of TM-mediated inhibition of tumor metastasis. Our results suggest that TM treatment significantly inhibits HNSCC metastasis by decreasing tumor cell motility by inhibiting lysyl oxidase and focal adhesion kinase. In addition, TM treatment inhibited tumor cell invasiveness by down-regulating MMP2 levels. Moreover, TM treatment also significantly enhanced tumor cell anoikis by activating p38 MAPK cell death pathway and downregulating XIAP survival proteins.

## METHODS

**Cell cultures.** Primary human dermal microvascular endothelial cells (ECs) were purchased from Lonza (Walkersville, MD). ECs were maintained in Endothelial Cell Basal Medium-2 (EBM-2) containing 5% FBS and growth supplements. Oral squamous carcinoma cells (OSCC-3, a kind gift from M. Lingen, University of Chicago) were maintained in Dulbecco's Modified Eagle Medium (DMEM) supplemented with 10% FBS.

**Transduction of endothelial cells with Bcl-2.** Bcl-2 was introduced into human microvascular endothelial cells (ECs) as described previously [32]. The Bcl-2 construct or the vector alone was introduced into PA317 amphotropic packing cells with Lipofectin. Viral supernatants were collected after 24 hours, centrifuged, filtered, and stored at -70$^{o}$C. ECs were transduced with either Bcl-2 (EC-Bcl-2) or control vector (EC-VC) by overnight incubation with one-tenth dilution of the viral supernatant in the presence of 6 μg/ml polybrene. Transduced ECs were selected by treating them with G418 (200 μg/ml) for one week. Bcl-2 expression in endothelial cells was confirmed by Western blot analysis.

**Generation of oral squamous cell line stably expressing luciferase**. Tumor cells (OSCC-3) were transfected with pcDNA3.1 plasmid containing the firefly luciferase gene [33] (a gift from Dr. Alnawaz Rehemtulla, University of Michigan, Ann Arbor) using Lipofectamine 2000 as described previously [34]. Four μg of each plasmid and 20 μl of Lipofectamine 2000 reagent were separately diluted in 200 μl of DMEM and incubated for 45 minutes at room temperature. The two solutions were gently mixed and further incubated for 15 minutes at room temperature to prepare the lipid-DNA complexes. Subsequently, 1.6 ml of DMEM containing 5% FBS was gently mixed with lipid-DNA complexes. Tumor cells were washed twice with DMEM and then lipid-DNA complexes were overlaid onto the cells. The cells were incubated for 6 hours at 37$^{o}$C

in a $CO_2$ incubator. At the end of the incubation, DNA containing medium was removed and replaced with DMEM. Luciferase transduced OSCC-3 (OSCC-3-Luc) cells were selected by incubating in DMEM containing 400 µg/ml G418 for 7 days.

**Tumor metastasis models.** We used two *in vivo* models (flank xenograft and tail vein injection models) to study the effects of TM on tumor metastasis.

SCID mouse flank xenograft model. Six weeks old female SCID mice were used in this study. Animals were randomized to receive either TM or sterilized water, delivered daily p.o. gavaging. The treatment was initiated 2 weeks prior to the tumor inoculation and continued until the end of the experiment. Plasma ceruloplasmin is a good surrogate marker for total body copper status therefore ceruloplasmin levels were measured using oxidase assay as described before [25]. The baseline levels of plasma ceruloplasmin were determined for the TM group before initiation of treatment. Subsequently, ceruloplasmin levels were measured biweekly over the study periods. TM treatment was started at 0.7 mg/day per mouse and then titrated biweekly to maintain ceruloplasmin suppression at 20% to 30% of baseline. OSCC-3-Luc ($1 \times 10^6$) and endothelial cells (EC-VC or EC-Bcl-2, $1 \times 10^6$) were mixed with 100 µl of Matrigel and injected subcutaneously in the flanks of SCID mice [14]. Tumor volume measurements began on day 3 and continued twice a week until the end of the study. The length and width of the tumors were measured using a digital caliper and tumor volumes were calculated using the formula, volume ($mm^3$) = $L \times W^2/2$ (length L, mm; width W, mm). After 3 weeks, primary tumors and lungs were carefully removed and analyzed for tumor growth, tumor angiogenesis and tumor metastasis to lungs. Lungs from each mouse were divided into two parts. One half of each lung was fixed with 10% buffered formalin and then processed to form paraffin embedded tissue blocks for immunohistochemistry. The other half of the lung was used to harvest tumor cells. Lungs were

finely minced by scissors, washed with sterile serum free media (DMEM) and treated with collagenase (2.5 mg/ml) for 3 hours at 37$^{o}$C with intermittent shaking. After collagenase treatment, cells were plated in 10 cm culture dishes and treated with G418 (400 μg/ml) to select tumor cells (OSCC-3-Luc). After one week, tumor cell colonies were counted using phase contrast microscope (50x).

Tail vein metastasis model. In this study, SCID mice were treated with TM as described above. OSCC-3-Luc cells (0.5 x10$^{5}$) in 50 μl volume were injected in the SCID mice via tail vein using 30 gauge needles. Tumor metastasis to lungs was monitored by *in vivo* bioluminescence imaging. After 3 weeks, lungs were carefully removed and tumor metastasis to lungs was analyzed as described above.

***In vivo* Bioluminescence Imaging.** Mice were imaged on a cryogenically cooled imaging system (Xenogen, Alameda, CA, USA) coupled to a data acquisition computer. Mice were anesthetized (1.5% Isoflurane/air mixture), and injected with luciferin in PBS at a dose of 320 mg/kg body weight. Digital gray images were captured and overlaid with pseudocolor images, which represent photon counts emitted from active luciferase within viable tumor cells. Luminescence emitted from each animal was integrated for one-minute intervals, from 5-20 minutes after the injection of Luciferin. Image processing and photon count quantitation were conducted by means of Living Image software (Xenogen).

**Quantitaion of angiogenesis by immunolocalization of von Willebrand Factor.** Tissue sections were deparaffinized and antigen retrieval was achieved by pressure cooking in a Decloaking chamber (Biocare Medical, Walnut Creek, CA) at 120$^{o}$C for 20 minutes [35]. Tissue sections were then treated with peroxide block solution for 5 minutes at room temperature followed by 1 hour of incubation with primary antibody (anti-von Willebrand Factor, Dako,

Carpinteria, CA) at room temperature. Slides were further incubated for 30 minutes with HRP labeled polymer (Dako EnVision+ Kit, Carpinteria, CA) and developed with AEC+chromagen. Microvessel density was calculated by counting 5 random high power fields (200x).

**Tumor cell motility assay.** Random cell motility was determined using a motility assay kit (Cellomics, Pittsburgh, PA) as per manufacturer's instructions. In brief, OSCC-3 cells were harvested, suspended in serum-free medium and plated on top of a field of microscopic fluorescent beads in the presence or absence of TM (1 nM). After a 16-hours incubation period, cells were fixed and areas of clearing in the fluorescent bead field corresponding to phagokinetic cell tracks were quantified using NIH ScionImager.

**Lysyl oxidase (LOX) activity assay.** LOX activity of whole-cell lysates was measured using the Amplex Red fluorescence assay kit (Molecular Probes, Eugene, OR). The assay reaction mixture consisted of 50 mM sodium borate (pH 8.2), 1.2 M urea, 50 μM Amplex Red, 0.1 units/ml horseradish peroxidase, and 10 mM 1,5-diaminopentane substrate. TM treated or untreated control protein samples were added to the reaction mixture and incubated at 37$^{o}$C. The fluorescence intensity was measured every 30 minutes for 2 hours using a Synergy 4 multidetection microplate reader (BioTek, Winooski, VT). LOX activity is expressed as fluorescent units.

**Western Blot Analysis.** OSCC-3 cells were cultured in 6-well plates and treated with TM for different time points. Whole cell lysates were separated by 4-12% NuPAGE Bis-Tris gels (Invitrogen, Carlsbad, CA) and transferred onto nitrocellulose membranes using NuPAGE transfer buffer (Invitrogen, Carlsbad, CA). To block nonspecific binding, membranes were incubated with 5% non-fat milk in Tris buffered saline containing 0.1% Tween-20 (TBST) for 1 hour at room temperature. Afterwards, the blots were incubated in the respective primary

antibody in TBST + 5% non-fat milk at 4°C overnight. After washing with TBST, the blots were incubated with horseradish peroxidase-conjugated sheep anti-mouse IgG (1:10,000) or with goat anti-rabbit IgG (1:10,000) for 1 hour at room temperature. An ECL-plus detection system (Amersham Life Sciences, Piscataway, NJ) was used to detect specific protein bands. Protein loading in all the experiments was normalized by stripping the blots and then re-probing with anti-tubulin antibody.

**Tumor cell invasion assays.** The role of TM in tumor cell invasion was investigated using a Matrigel invasion assay [14]. 24-well plate inserts (8 μM pore size, Falcon) were coated with 20 μl of Matrigel and incubated at 37°C for 30 minutes to let the Matrigel polymerize. Next, 50,000 tumor cells (OSCC-3) were carefully layered on top of the Matrigel and the inserts were placed in the 24 well plates in the presence or absence of TM (1 nM). The plates were further incubated for 24 hours at 37°C and the non-invaded cells were carefully removed with a cotton swab. The inserts were then stained with Diff-quick solution II and mounted on glass slides. The number of cells that had invaded through the Matrigel was counted in 5 high power fields.

**MMP analysis by zymography.** OSCC-3 cells ($5x10^5$) were cultured in a 6-well plate. Separately, EC-VC or EC-Bcl-2 ($5x10^5$) cells were plated on top of collagen coated inserts and then these inserts were carefully placed in the 6-well plates containing OSCC-3 cells in the presence or absence of TM (1 nM). After 24 hours, OSCC-3 cells were washed and further cultured in serum free media (DMEM) for 24 hours. At the end of incubation, culture supernatants were collected and mixed with non-reducing SDS gel sample buffer (3:1) and applied without boiling to a 10% polyacrylamide gelatin gel (Invitrogen, Carlsbad, CA). After electrophoresis, the gels were washed with $ddH_2O$ and incubated in renaturing buffer (50 mM Tris-HCl, pH 7.5) containing 2% Triton X-100 for 30 minutes at room temperature, and then incubated in developing buffer (50 mM Tris-HCl, pH 7.5) containing 5 mM $CaCl_2$ and 1 M $ZnCl_2$ at 37°C for 16 hours. Gels were stained by 0.5% Coomassie Brilliant Blue R-250 solution

to visualize the bands. The band density was measured using Alpha Imager software (Alpha Innotech, San Leandro, CA).

**Tumor cell anoikis assay.** To evaluate the tumor cell anoikis in non-adherent conditions, OSCC-3 cells ($5x10^5$) were cultured in a 6-well plate over a thick layer of 1% agar in DMEM containing 2% serum. Tumor cells cultured in adherent conditions were used as a control. In the TM treatment experiments, tumor cells were pre-treated with TM (1nM) for 24 hours and then cultured on top of 1% agar. At the end of incubation, cells were carefully retrieved and analyzed by TUNEL staining for anoikis [12]. In brief, tumor cells were fixed with cytofix buffer (BD cytofix, BD Biosciences, San Jose, CA) for 15 minutes at $4^oC$, and then stored overnight in 70% ethanol at $-20^oC$. The percentage of apoptotic cells were then evaluated using the APO-BRDU terminal deoxynucleotidyl transferase (TdT)-mediated dUTP-biotin nick end labeling (TUNEL) assay according to the manufacturer's instructions (Sigma, St. Louis, MO). Apoptotic tumor cells were quantitated by flow cytometry using an argon laser excited at 488 nm (BD Biosciences, San Jose, CA).

**Statistical analysis.** Data from all the experiments are expressed as mean $\pm$ SEM. Statistical differences were determined by two-way analysis of variance and Student's t test. A p value of $<0.05$ was considered significant.

## RESULTS

**TM treatment significantly inhibited EC-Bcl-2 mediated tumor growth and angiogenesis.** We have previously shown that elevated expression of Bcl-2 in tumor-associated endothelial cells directly correlates with tumor metastasis in head and neck cancer patients [14]. In addition, we also demonstrated that co-implantation of EC-Bcl-2 along with oral squamous carcinoma cells (OSCC-3) in SCID mice significantly enhances tumor growth and tumor metastasis to lungs. In this study, we examined if treatment with an anti-angiogenic agent (tetrathiomolybdate, TM) could inhibit tumor growth and tumor angiogenesis in this aggressive squamous cell carcinoma model. The level of plasma ceruloplasmin, which is a good surrogate marker for total body copper status, was monitored biweekly and TM dose was adjusted accordingly to maintain ceruloplasmin suppression at 20% to 30% of baseline. OSCC-3 tumors containing EC-Bcl-2 showed significantly higher tumor growth (Fig. 1A) as compared to OSCC-3 tumors containing endothelial cells with vector alone (EC-VC). In addition, OSCC-3 tumors containing EC-Bcl-2 showed significantly higher tumor weight (Fig. 1B) at the end of study as compared to OSCC-3 containing EC-VC. TM treatment significantly inhibited tumor growth and tumor weights in OSCC-3 tumor containing EC-Bcl-2. In addition, TM treatment significantly inhibited blood vessel density in OSCC-3 tumors containing EC-Bcl-2 cells (Fig. 1C-D). TM treatment did not cause any animal mortality or induce significant decrease in body weight (less than 5% weight loss in TM treatment as compared control, data not shown). TM treatment also did not induce any systemic toxicity such as respiratory depression or dry scaly skin.

**TM treatment significantly inhibited tumor metastasis to lungs.** We used two *in vivo* models (flank xenograft and tail vein injection models) to examine if TM treatment could inhibit tumor metastasis. OSCC-3 tumors populated with EC-Bcl-2 showed significantly higher metastasis to

lungs as compared to OSCC-3 tumors populated with EC-VC (Fig. 2). In addition to higher number of metastatic nodules, OSCC-3 tumors containing EC-Bcl-2 also had larger lung metastasis nodes (Fig. 2B). Lungs harvested from animals co-implanted with OSCC-3 and EC-Bcl-2 showed significantly higher number of colonies and contained significantly higher number of cells as compared to OSCC-3 and EC-VC group. TM treated animals showed significantly lower number of tumor cell colonies and cells (Fig. 2C-D).

In the tail vein metastasis model, TM treatment markedly inhibited tumor metastasis to lungs at both day 16 and 21 (Fig. 3A-B). Similarly, lungs harvested from TM treated animals showed significantly lower number of colonies and tumor cells (Fig. 3C-D).

**TM treatment markedly reduced oral squamous cell motility and invasiveness.** Tumor cells cultured in the presence of serum (S+) exhibited significantly higher motility as compared to tumor cells cultured in the absence of serum (S-). TM treatment significantly inhibited tumor cell motility both in the presence (S+TM+) and absence (S-TM+) of serum (Fig. 4A-B). Lysyl oxidase (LOX), a copper-dependent amine oxidase, has been shown to promote tumor cell migration and invasion. [24]. We next examined if TM mediated its inhibitory effect on tumor cell motility by inhibiting LOX. Indeed, TM treatment of OSCC-3 cells significantly inhibited LOX activity (Fig. 4C). In addition, TM also inhibited the activation of focal adhesion kinase (FAK), an important cell migration mediator (Fig. 4D).

In the next set of experiments, we examined if TM affects OSCC-3 cell invasiveness. TM treatment significantly inhibited OSCC-3 invasiveness (Fig. 5A-B). Matrix matelloproteinases (MMPs) plays an important role in tumor cell invasiveness by degrading extracellular matrix. We also examined whether EC-Bcl-2 cells could enhance MMPs production by OSCC-3 cells and if TM treatment could inhibit the secretion of MMPs. OSCC-3 cells co-cultured with EC-

Bcl-2 showed significant increase in MMP2 secretion as compared to OSCC-3 cells co-cultured with EC-VC (Fig. 5A-B). TM treatment of EC-Bcl-2 and OSCC-3 significantly inhibited MMP2 production (Fig. 5C-D).

**TM treatment significantly inhibited tumor cell anoikis.** In our tail vein metastasis model, we observed significant inhibition of tumor metastasis in TM treated animals. We further examined if TM inhibits tumor metastasis in tail vein model by promoting tumor cell anoikis. TM treatment significantly enhanced tumor cell anoikis in a time dependent manner (Fig 6A). Interestingly, TM had no effect on adherent OSCC-3 cells (Fig 6A). Survival proteins XIAP and Bcl-2 play an important role in anoikis resistance. We next examined if TM treatment downregulates the expression of these survival proteins in non-adherent conditions. TM treatment markedly downregulated XIAP protein expression in a time dependent manner (Fig. 6B). However, TM treatment did not alter the Bcl-2 expression (data not shown). Moreover, TM treatment also activated stress activated p38 MAPK cell death signaling pathway (Fig. 6B).

## DISCUSSION

Distant metastases in head and neck cancer almost invariably herald a poor prognosis with an average survival of 6 months and treatment is usually palliative [36]. Five year survival rates for early stage localized head and neck cancers are over 80% but this drop to 40% where disease has spread to neck nodes, and to below 20% for patients with distant metastatic disease [37]. Currently used treatment regimens (surgery and/or chemo-radiation) are often ineffective in controlling the metastatic spread of disease [3]. It is therefore very important to develop novel therapies for patients with metastatic disease. Copper is a mandatory cofactor for a number of proteins that play an important role in angiogenesis, tumor cell migration and survival [38]. We have previously shown that TM, a potent copper chelator, inhibits tumor growth and tumor metastasis by suppressing angiogenesis [29]. Recently, Juarez et al, have shown that TM attenuates angiogenesis and tumor cell proliferation by inhibiting superoxide dismutase 1 (SOD1) [30]. However, very little is known about the role of TM on key metastatic processes, particularly tumor cell migration, invasion and anoikis resistance. In this study, we have examined the mechanisms by which TM inhibits tumor cell motility, invasiveness and anoikis resistance.

We used two *in vivo models* (flank xenograft model and tail vein model) to test the efficacy of TM in inhibiting tumor metastasis. In the first *in vivo* model, oral squamous carcinoma cells (OSCC-3) were co-implanted along with endothelial cells expressing Bcl-2 (EC-Bcl-2) in the flanks of SCID mice [14]. The rationale for co-implanting EC-Bcl-2 along with OSCC-3 is based on our previous work where we have demonstrated that co-implantation of EC-Bcl-2 along with tumor cells significantly enhances tumor metastasis. In addition, these EC-Bcl-2 containing tumors exhibited highly invasive phenotype and abnormal vascular network as

commonly observed with aggressive human tumors. Therefore, this highly aggressive xenograft model is ideally suited to test the efficacy of TM on tumor metastasis. Our results suggest that TM inhibits tumor metastasis by blocking multiple steps that are involved in tumor metastasis cascade (tumor cell migration, invasion and survival in circulation) to reach the distal site.

Tumor cell motility and invasiveness are key characteristics of aggressive metastatic tumors as they play an important role in tumor cell release from the primary tumors into the circulation. To examine if TM treatment affects tumor cell motility, we used a random cell motility assay. TM treatment significantly inhibited tumor cell motility both in the presence and in the absence of serum. Cell migration is a dynamic process that is regulated by the formation or turnover of focal contacts. Focal adhesion kinase (FAK) is the key member of the focal contact assembly and FAK activation is required for optimal cell motility [39]. TM treatment significantly inhibited FAK activation as well as the activation of LOX. LOX, a copper-dependent amine oxidase, was initially reported as responsible for the catalysis of collagen and elastin cross-linking within the extracellular matrix [40]. However, recent work has shown that LOX regulates a number of cellular functions including cell migration via the activation of FAK/Src pathway [41] [24]. Therefore, TM may be inhibiting tumor cell migration by inhibiting FAK activation via lysyl oxidase. We further examined the role of TM in tumor cell invasiveness by using Matrigel invasion assay. TM treatment significantly inhibited oral squamous cell invasion through Matrigel. Matrix metalloproteinases (MMPs) play an important role in tumor cell invasiveness by digesting the extracellular matrix. In HNSCC, MMP-2 and MMP-9 have been shown to be involved in tumor cell invasion [42, 43]. Our results demonstrate that tumor cells co-cultured with EC-Bcl-2 showed marked increase in activated MMP-2 as compared to tumor cells co-cultured with EC-VC. TM treatment of OSCC-3 and EC-Bcl-2 significantly

inhibited MMP-2 production. This TM-mediated decrease in MMP-2 production could be due to its inhibitory effect on FAK as it has been shown that blocking of FAK activity by either dominant negative mutants or antisence treatment significantly decreases MMP expression [44, 45].

Once the tumor cells invade through the matrix to enter the circulation, they have to survive the harsh circulatory conditions to successfully metastasize to distal sites. We next examined if TM treated affect tumor cell survival in circulation by using tail vein metastasis model. TM treatment significantly inhibited tumor metastasis to lungs in the SCID mouse model. To further examine if TM treatment promotes tumor cell death (anoiks) in non-adhering conditions, we cultured OSCC-3 cells on top of 1% agar in the presence or absence of TM. TM treatment significantly enhanced tumor cell anoikis. Interestingly, TM treatment did not affect OSCC-3 survival in adherent condition. TM could be promoting tumor cell anoikis by increasing oxidative stress (p38 MAPK activation) in the cells by down modulating superoxide dismutase (SOD) and X-linked inhibitor of apoptosis (XIAP) , as copper is a cofactor for both SOD and XIAP proteins [30, 46]. SOD protects cells from oxidative stress by catalyzing the disproportionation of superoxide to hydrogen peroxide [47], whereas XIAP protein modulates oxidative stress by binding to apoptosis-inducing factor (AIF) [46]. In addition, XIAP has been shown to promote cell survival by directly binding to caspase 3 and inhibiting its function by blocking substrate binding [48].

## CONCLUSIONS

In conclusion, our results demonstrate that TM significantly inhibits head and neck tumor metastasis by modulating a number of critical steps involved in tumor metastasis cascade including angiogenesis, tumor cell motility, invasiveness and tumor cell anoikis. Therefore, TM

with its low toxicity profile and good oral bioavailability is a potentially novel candidate to control tumor metastasis in head and neck cancer patients.

**List of abbreviations used:** HNSCC, head and neck squamous cell carcinoma; OSCC-3, oral squamous cell carcinoma-3; EC, endothelial cell; TM, tetrathiomolybdate; FAK, focal adhesion kinase; LOX, lysyl oxidase; XIAP, X-linked Inhibitor of Apoptosis Protein; VEGF, vascular endothelial cell growth factor; SCID, Severe combined immunodeficiency disease; MMP, Matrix metalloproteinases.

**Competing interests:** Dr. Merajver has equity and was a consultant for Attenuon, LLC, an entity which has licensed tetrathiomolybdate for anti-angiogenic applications from the University of Michigan.

**Authors' contribution:** PK conceived of the study, participated in the design, carried out some of the *in vivo*, anoikis & invasion studies, and drafted the manuscript. AY carried out the molecular mechanistic studies. SP carried out *in vivo* studies. MI carried out the immunohistochemistry. QP carried out tumor cell motility studies, SDM participated in the design and coordination of the studies. TNT participated in conceiving, design and coordination of the studies. All authors red and approved the final version.

**Acknowledgements:** We thank Dr. M. Lingen (University of Chicago) for providing OSCC-3 cell line and Dr. A. Rehemtulla (University of Michigan) for providing pcDNA3.1 luciferase plasmid. This work was funded by National Cancer Institute SPORE grants P50CA97248 (PK, TNT and SDM), NCI K-Award CA133250 (PK), NIH CA77612 (SDM) and by the Breast Cancer Research Foundation (SDM).

## REFERENCES


1. Ragin CC, Modugno F, Gollin SM: **The epidemiology and risk factors of head and neck cancer: a focus on human papillomavirus.** *J Dent Res* 2007, **86:**104-114.
2. Jemal A, Thomas A, Murray T, Thun M: **Cancer statistics, 2002.** *CA Cancer J Clin* 2002, **52:**23-47.
3. Deschamps DR, Spencer HJ, Kokoska MS, Spring PM, Vural EA, Stack BC, Jr.: **Implications of head and neck cancer treatment failure in the neck.** *Otolaryngol Head Neck Surg*, **142:**722-727.
4. Ferlito A, Shaha AR, Silver CE, Rinaldo A, Mondin V: **Incidence and Sites of Distant Metastases from Head and Neck Cancer.** *ORL* 2001, **63:**202-207.
5. Teknos TN, Islam M, Arenberg DA, Pan Q, Carskadon SL, Abarbanell AM, Marcus B, Paul S, Vandenberg CD, Carron M, et al: **The effect of tetrathiomolybdate on cytokine expression, angiogenesis, and tumor growth in squamous cell carcinoma of the head and neck.** *Arch Otolaryngol Head Neck Surg* 2005, **131:**204-211.
6. Lathers DM, Young MR: **Increased aberrance of cytokine expression in plasma of patients with more advanced squamous cell carcinoma of the head and neck.** *Cytokine* 2004, **25:**220-228.
7. Chen Z, Malhotra PS, Thomas GR, Ondrey FG, Duffey DC, Smith CW, Enamorado I, Yeh NT, Kroog GS, Rudy S, et al: **Expression of proinflammatory and proangiogenic cytokines in patients with head and neck cancer.** *Clin Cancer Res* 1999, **5:**1369-1379.
8. Smith BD, Smith GL, Carter D, Sasaki CT, Haffty BG: **Prognostic significance of vascular endothelial growth factor protein levels in oral and oropharyngeal squamous cell carcinoma.** *J Clin Oncol* 2000, **18:**2046-2052.
9. Masuda M, Ruan HY, Ito A, Nakashima T, Toh S, Wakasaki T, Yasumatsu R, Kutratomi Y, Komune S, Weinstein IB: **Signal transducers and activators of transcription 3 up-regulates vascular endothelial growth factor production and tumor angiogenesis in head and neck squamous cell carcinoma.** *Oral Oncol* 2007, **43:**785-790.
10. Sauter ER, Nesbit M, Watson JC, Klein-Szanto A, Litwin S, Herlyn M: **Vascular endothelial growth factor is a marker of tumor invasion and metastasis in squamous cell carcinomas of the head and neck.** *Clin Cancer Res* 1999, **5:**775-782.
11. Teknos TN, Cox C, Yoo S, Chepeha DB, Wolf GT, Bradford CR, Carey TE, Fisher SG: **Elevated serum vascular endothelial growth factor and decreased survival in advanced laryngeal carcinoma.** *Head Neck* 2002, **24:**1004-1011.
12. Kumar P, Miller AI, Polverini PJ: **p38 MAPK mediates gamma-irradiation-induced endothelial cell apoptosis, and vascular endothelial growth factor protects endothelial cells through the phosphoinositide 3-kinase-Akt-Bcl-2 pathway.** *J Biol Chem* 2004, **279:**43352-43360.
13. Kumar P, Coltas IK, Kumar B, Chepeha DB, Bradford CR, Polverini PJ: **Bcl-2 protects endothelial cells against gamma-radiation via a Raf-MEK-ERK-survivin signaling pathway that is independent of cytochrome c release.** *Cancer Res* 2007, **67:**1193-1202.
14. Kumar P, Ning Y, Polverini PJ: **Endothelial cells expressing Bcl-2 promotes tumor metastasis by enhancing tumor angiogenesis, blood vessel leakiness and tumor invasion.** *Lab Invest* 2008, **88:**740-749.

15. Ahmad A, Hart IR: **Mechanisms of metastasis.** *Crit Rev Oncol Hematol* 1997, **26:**163-173.
16. Manes S, Mira E, Gomez-Mouton C, Lacalle RA, Martinez C: **Cells on the move: a dialogue between polarization and motility.** *IUBMB Life* 2000, **49:**89-96.
17. Maung K, Easty DJ, Hill SP, Bennett DC: **Requirement for focal adhesion kinase in tumor cell adhesion.** *Oncogene* 1999, **18:**6824-6828.
18. Schneider GB, Kurago Z, Zaharias R, Gruman LM, Schaller MD, Hendrix MJ: **Elevated focal adhesion kinase expression facilitates oral tumor cell invasion.** *Cancer* 2002, **95:**2508-2515.
19. Hauck CR, Sieg DJ, Hsia DA, Loftus JC, Gaarde WA, Monia BP, Schlaepfer DD: **Inhibition of focal adhesion kinase expression or activity disrupts epidermal growth factor-stimulated signaling promoting the migration of invasive human carcinoma cells.** *Cancer Res* 2001, **61:**7079-7090.
20. Talvensaari-Mattila A, Pääkkö P, Höyhtyä M, Blanco-Sequeiros G, Turpeenniemi-Hujanen T: **Matrix metalloproteinase-2 immunoreactive protein.** *Cancer* 1998, **83:**1153-1162.
21. Väisänen A, Kallioinen M, Taskinen PJ, Turpeenniemi-Hujanen T: **Prognostic value of MMP-2 immunoreactive protein (72 kD type IV collagenase) in primary skin melanoma.** *The Journal of Pathology* 1998, **186:**51-58.
22. Ruokolainen H, Paakko P, Turpeenniemi-Hujanen T: **Tissue and circulating immunoreactive protein for MMP-2 and TIMP-2 in head and neck squamous cell carcinoma[mdash]tissue immunoreactivity predicts aggressive clinical course.** *Mod Pathol* 2005, **19:**208-217.
23. Duxbury MS, Ito H, Zinner MJ, Ashley SW, Whang EE: **Focal adhesion kinase gene silencing promotes anoikis and suppresses metastasis of human pancreatic adenocarcinoma cells.** *Surgery* 2004, **135:**555-562.
24. Payne SL, Fogelgren B, Hess AR, Seftor EA, Wiley EL, Fong SF, Csiszar K, Hendrix MJ, Kirschmann DA: **Lysyl oxidase regulates breast cancer cell migration and adhesion through a hydrogen peroxide-mediated mechanism.** *Cancer Res* 2005, **65:**11429-11436.
25. Brewer GJ: **Copper control as an antiangiogenic anticancer therapy: lessons from treating Wilson's disease.** *Exp Biol Med (Maywood)* 2001, **226:**665-673.
26. Pan Q, Kleer CG, van Golen KL, Irani J, Bottema KM, Bias C, De Carvalho M, Mesri EA, Robins DM, Dick RD, et al: **Copper deficiency induced by tetrathiomolybdate suppresses tumor growth and angiogenesis.** *Cancer Res* 2002, **62:**4854-4859.
27. McAuslan BR, Reilly W: **Endothelial cell phagokinesis in response to specific metal ions.** *Exp Cell Res* 1980, **130:**147-157.
28. Hu GF: **Copper stimulates proliferation of human endothelial cells under culture.** *J Cell Biochem* 1998, **69:**326-335.
29. Hassouneh B, Islam M, Nagel T, Pan Q, Merajver SD, Teknos TN: **Tetrathiomolybdate promotes tumor necrosis and prevents distant metastases by suppressing angiogenesis in head and neck cancer.** *Mol Cancer Ther* 2007, **6:**1039-1045.
30. Juarez JC, Betancourt O, Jr., Pirie-Shepherd SR, Guan X, Price ML, Shaw DE, Mazar AP, Donate F: **Copper binding by tetrathiomolybdate attenuates angiogenesis and tumor cell proliferation through the inhibition of superoxide dismutase 1.** *Clin Cancer Res* 2006, **12:**4974-4982.

31. Goodman VL, Brewer GJ, Merajver SD: **Control of copper status for cancer therapy.** *Curr Cancer Drug Targets* 2005, **5:**543-549.
32. Nor JE, Christensen J, Liu J, Peters M, Mooney DJ, Strieter RM, Polverini PJ: **Up-Regulation of Bcl-2 in microvascular endothelial cells enhances intratumoral angiogenesis and accelerates tumor growth.** *Cancer Res* 2001, **61:**2183-2188.
33. Zhang L, Lee KC, Bhojani MS, Khan AP, Shilman A, Holland EC, Ross BD, Rehemtulla A: **Molecular imaging of Akt kinase activity.** *Nat Med* 2007, **13:**1114-1119.
34. Kumar P, Amin MA, Harlow LA, Polverini PJ, Koch AE: **Src and phosphatidylinositol 3-kinase mediate soluble E-selectin-induced angiogenesis.** *Blood* 2003, **101:**3960-3968.
35. Kumar P, Benedict R, Urzua F, Fischbach C, Mooney D, Polverini P: **Combination treatment significantly enhances the efficacy of antitumor therapy by preferentially targeting angiogenesis.** *Lab Invest* 2005, **85:**756-767.
36. Ferlito A, Rinaldo A, Buckley JG, Mondin V: **General Considerations on Distant Metastases from Head and Neck Cancer.** *ORL* 2001, **63:**189-191.
37. Kalavrezos N, Bhandari R: **Current trends and future perspectives in the surgical management of oral cancer.** *Oral Oncol*, **46:**429-432.
38. Turski ML, Thiele DJ: **New roles for copper metabolism in cell proliferation, signaling, and disease.** *J Biol Chem* 2009, **284:**717-721.
39. Schlaepfer DD, Mitra SK: **Multiple connections link FAK to cell motility and invasion.** *Curr Opin Genet Dev* 2004, **14:**92-101.
40. Kagan HM, Li W: **Lysyl oxidase: properties, specificity, and biological roles inside and outside of the cell.** *J Cell Biochem* 2003, **88:**660-672.
41. Lazarus HM, Cruikshank WW, Narasimhan N, Kagan HM, Center DM: **Induction of human monocyte motility by lysyl oxidase.** *Matrix Biol* 1995, **14:**727-731.
42. Patel BP, Shah SV, Shukla SN, Shah PM, Patel PS: **Clinical significance of MMP-2 and MMP-9 in patients with oral cancer.** *Head Neck* 2007, **29:**564-572.
43. Kawata R, Shimada T, Maruyama S, Hisa Y, Takenaka H, Murakami Y: **Enhanced production of matrix metalloproteinase-2 in human head and neck carcinomas is correlated with lymph node metastasis.** *Acta Otolaryngol* 2002, **122:**101-106.
44. Hauck CR, Hsia DA, Puente XS, Cheresh DA, Schlaepfer DD: **FRNK blocks v-Src-stimulated invasion and experimental metastases without effects on cell motility or growth.** *Embo J* 2002, **21:**6289-6302.
45. Zhang Y, Thant AA, Hiraiwa Y, Naito Y, Sein TT, Sohara Y, Matsuda S, Hamaguchi M: **A role for focal adhesion kinase in hyluronan-dependent MMP-2 secretion in a human small-cell lung carcinoma cell line, QG90.** *Biochem Biophys Res Commun* 2002, **290:**1123-1127.
46. Wilkinson JC, Wilkinson AS, Galban S, Csomos RA, Duckett CS: **Apoptosis-inducing factor is a target for ubiquitination through interaction with XIAP.** *Mol Cell Biol* 2008, **28:**237-247.
47. Rhee SG: **Cell signaling. H2O2, a necessary evil for cell signaling.** *Science* 2006, **312:**1882-1883.
48. Riedl SJ, Renatus M, Schwarzenbacher R, Zhou Q, Sun C, Fesik SW, Liddington RC, Salvesen GS: **Structural basis for the inhibition of caspase-3 by XIAP.** *Cell* 2001, **104:**791-800.

## Figure legends

**Figure 1. Tetrathiomolybdate (TM) treatment significantly inhibits HNSCC tumor growth and tumor angiogenesis.** OSCC-3 and EC-Bcl-2 or EC-VC cells were mixed with 100 µl of Matrigel and injected in the flanks of SCID mice. Tumor volume measurements began on day 3 and continued twice a week until the end of the study. Length and width were measured using a digital caliper and tumor volumes were calculated using the formula, volume ($mm^3$) = L x $W^2/2$ (length L, mm; width W, mm). **A;** tumor progression curves for different experimental groups: OSCC-3 plus endothelial cells transduced with vector alone (EC-VC); OSCC-3 plus endothelial cells transduced with vector alone and treated with TM (EC-VC+TM); OSCC-3 plus endothelial cells transduced with Bcl-2 (EC-Bcl-2); OSCC-3 plus endothelial cells transduced with Bcl-2 and treated with TM (EC-Bcl-2+TM). **B;** tumor weights at the end of the study. **C-D**; Paraffin embedded tumor sections were stained for tumor blood vessels using anti-human von Willebrand Factor antibodies. Microvessel density in the tumor samples was calculated by counting 5 random fields (x 200). *, represents a significant difference ($p<0.05$) as compared to the control group.

**Figure 2. TM treatment significantly inhibits EC-Bcl-2 mediated HNSCC tumor metastasis.** OSCC-3 and EC-Bcl-2 or EC-VC were mixed with 100 µl of Matrigel and injected in the flanks of SCID mice. Lungs from SCID mice were carefully removed on day 21. One half of each lung was fixed and paraffin embedded for immunohistochemical analysis. From the other half of the lung, tumor cells were harvested and selected by G418 treatment. **A;** representative gross lungs photomicrograph from different experimental groups. **B;** representative photomicrograph of lung sections from different experimental groups. **C;** Number of tumor cell

colonies present in different groups. **D;** Number of tumor cell present in different groups. *, represents a significant difference ($p<0.05$) as compared to the control group.

**Figure 3. TM treatment significantly inhibits HNSCC tumor metastasis.** OSCC-3-Luc cells were injected in the SCID mice via tail vein. Tumor metastasis to lungs was monitored by *in vivo* bioluminescence imaging. **A;** representative photomicrograph of animals treated with (TM+) or without TM (TM-) at days 16 and 21. **B;** Quantitative data of bioluminescence imagining as expressed as flux units. **C;** Tumor cells from lungs were harvested and tumor cell colonies were selected by G418 treatment (200 μg/ml) for one week and counted. **D;** Tumor cell colonies were then trypsinized and total number of cells were counted. *, represents a significant difference ($p<0.05$) as compared to the control group.

**Figure 4. TM treatment significantly inhibits oral squamous cell motility. A-B;** OSCC-3 cells were cultured on top of a field of microscopic fluorescent beads in the following culture conditions: in the absence of serum and TM (S-TM-); in the presence of serum but no TM (S+TM-); in the absence of serum but presence of TM (S-TM+) or in the presence of serum and TM (S+TM+). After a 16-hours incubation period, cells were fixed and areas of clearing in the fluorescent bead field corresponding to phagokinetic cell tracks were quantified using NIH ScionImager. **C;** LOX catalytic activity was measured in whole-cell lysates of untreated (NT) or TM treated OSCC-3 cells (30 minutes). *, represents a significant difference ($p<0.05$) as compared to the control group. **D;** Whole cell lysates of untreated or TM treated OSCC-3 cells were separated using 4-12% NuPAGE Bis-Tris gels and probed with anti-phospho-FAK antibody. Equal sample loading was verified by stripping the blots and re-probing with anti-tubulin antibody.

**Figure 5. TM treatment significantly inhibits oral squamous cell invasiveness.** TM effect on tumor cell invasiveness was examined by Matrigel invasion assay. **A;** representative photomicrographs of invaded cells with (TM+) or without TM (TM-) treatment. **B;** number of tumor cells that had invaded through the Matrigel were counted in 5 high power fields. *, represents a significant difference ($p<0.05$) as compared to the control group. **C;** Culture supernatants from OSCC-3 cells co-cultured with EC-Bcl-2 or EC-VC were resolved using 10% polyacrylamide gelatin gels. After electrophoresis, the gels were developed and stained by 0.5% Coomassie Brilliant Blue R-250 solution to visualize the bands. **D;** the band density was measured and expressed as average band density. *, represents a significant difference ($p<0.05$) as compared to the OSCC-3-EC-VC group and **, represents a significant difference ($p<0.05$) as compared to the OSCC-3-EC-Bcl-2 group.

**Figure 6. TM treatment significantly enhanced oral squamous cell anokis. A;** OSCC-3 cells were cultured either in normal adherent conditions (Ad) or non-adherent conditions (Non-Ad) for different time intervals. At the end of incubation, cells were carefully retrieved and analyzed by TUNEL staining for anoikis using flow cytometry. * represents a significant difference ($p<0.05$) as compared to the control group. **B;** OSCC-3 cells were cultured in non-adherent conditions for different time intervals. Whole cell lysates of untreated or TM treated OSCC-3 cells were separated using 4-12% NuPAGE Bis-Tris gels and probed with anti-phospho-p38MAPK, and XIAP antibody. Equal sample loading was verified by stripping the blots and re-probing with anti-tubulin antibody.

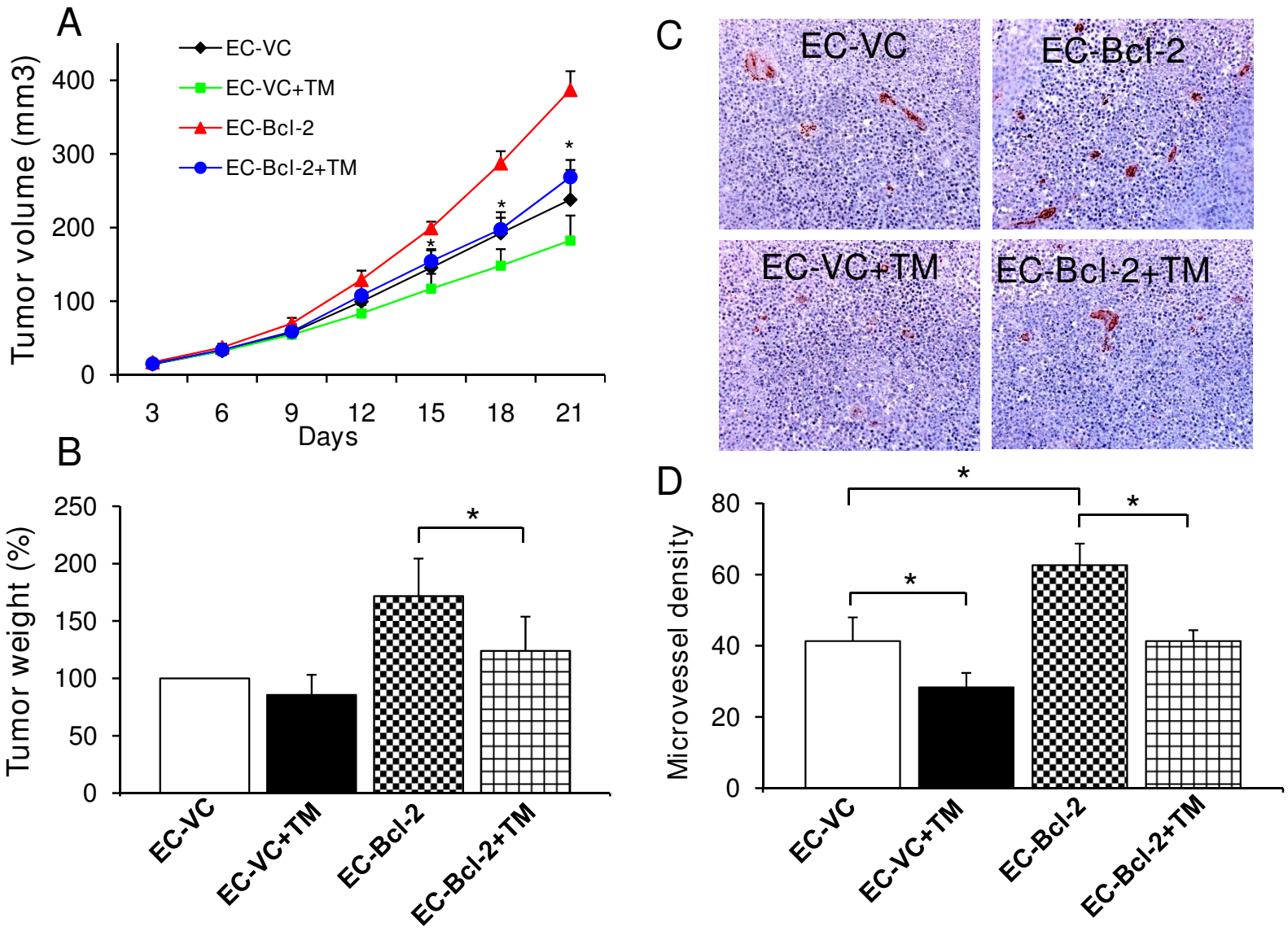
A
EC-VC
EC-VC+TM
EC-Bcl-2
EC-Bcl-2+TM
Tumor volume (mm3)
400
300
200
100
0
3
6
9
12
15
18
21
Days
*
*
*
B
Tumor weight (%)
250
200
150
100
50
0
*
EC-VC
EC-VC+TM
EC-Bcl-2
EC-Bcl-2+TM
C
EC-VC
EC-Bcl-2
EC-VC+TM
EC-Bcl-2+TM
D
Microvessel density
80
60
40
20
0
*
*
*
EC-VC
EC-VC+TM
EC-Bcl-2
EC-Bcl-2+TM

Figure 1

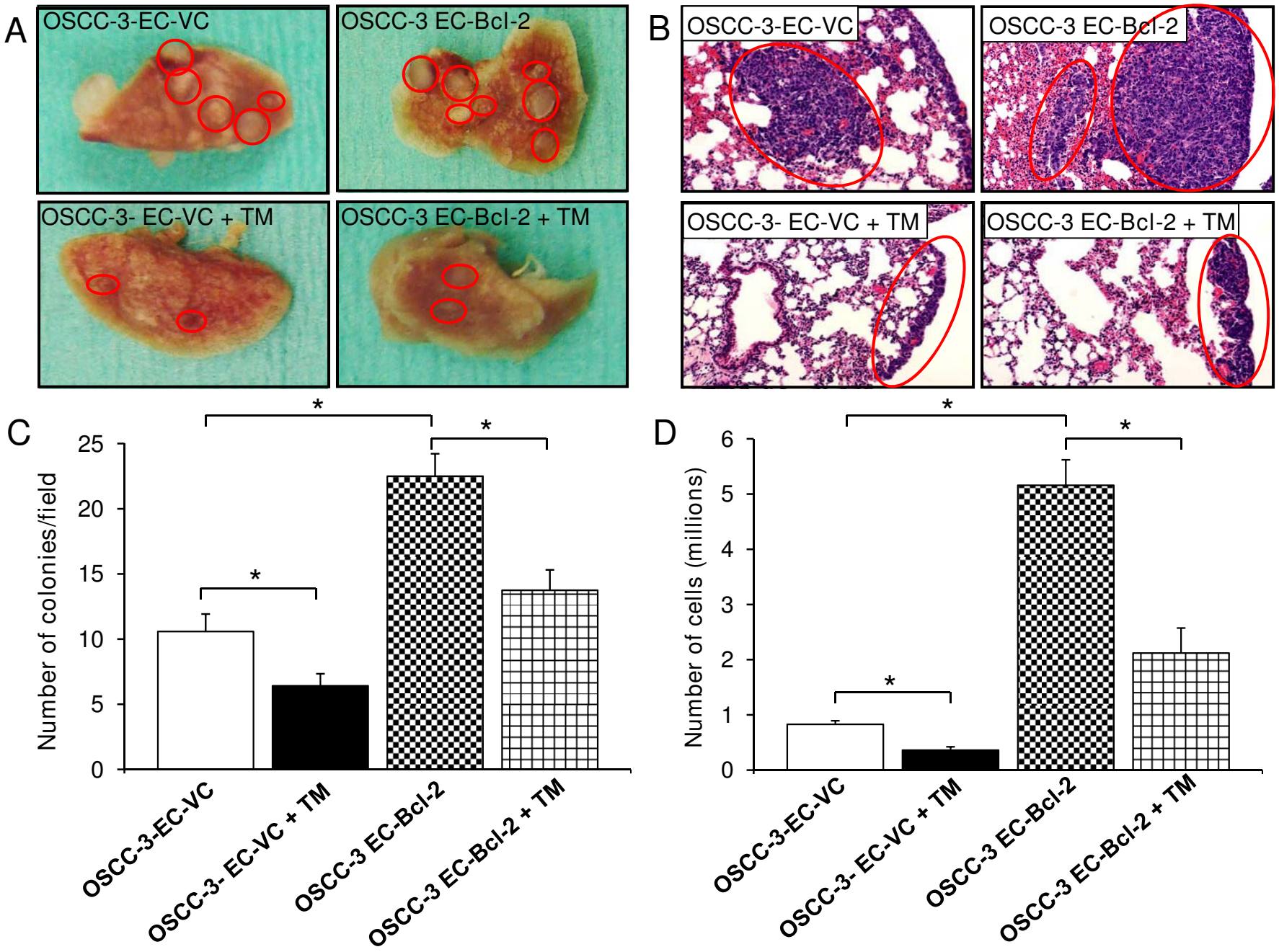
A
OSCC-3-EC-VC
OSCC-3 EC-Bcl-2
OSCC-3- EC-VC + TM
OSCC-3 EC-Bcl-2 + TM
B
OSCC-3-EC-VC
OSCC-3 EC-Bcl-2
OSCC-3- EC-VC + TM
OSCC-3 EC-Bcl-2 + TM
C
Number of colonies/field
0
5
10
15
20
25
*
*
*
OSCC-3-EC-VC
OSCC-3- EC-VC + TM
OSCC-3 EC-Bcl-2
OSCC-3 EC-Bcl-2 + TM
D
Number of cells (millions)
0
1
2
3
4
5
6
*
*
*
OSCC-3-EC-VC
OSCC-3- EC-VC + TM
OSCC-3 EC-Bcl-2
OSCC-3 EC-Bcl-2 + TM

Figure 2

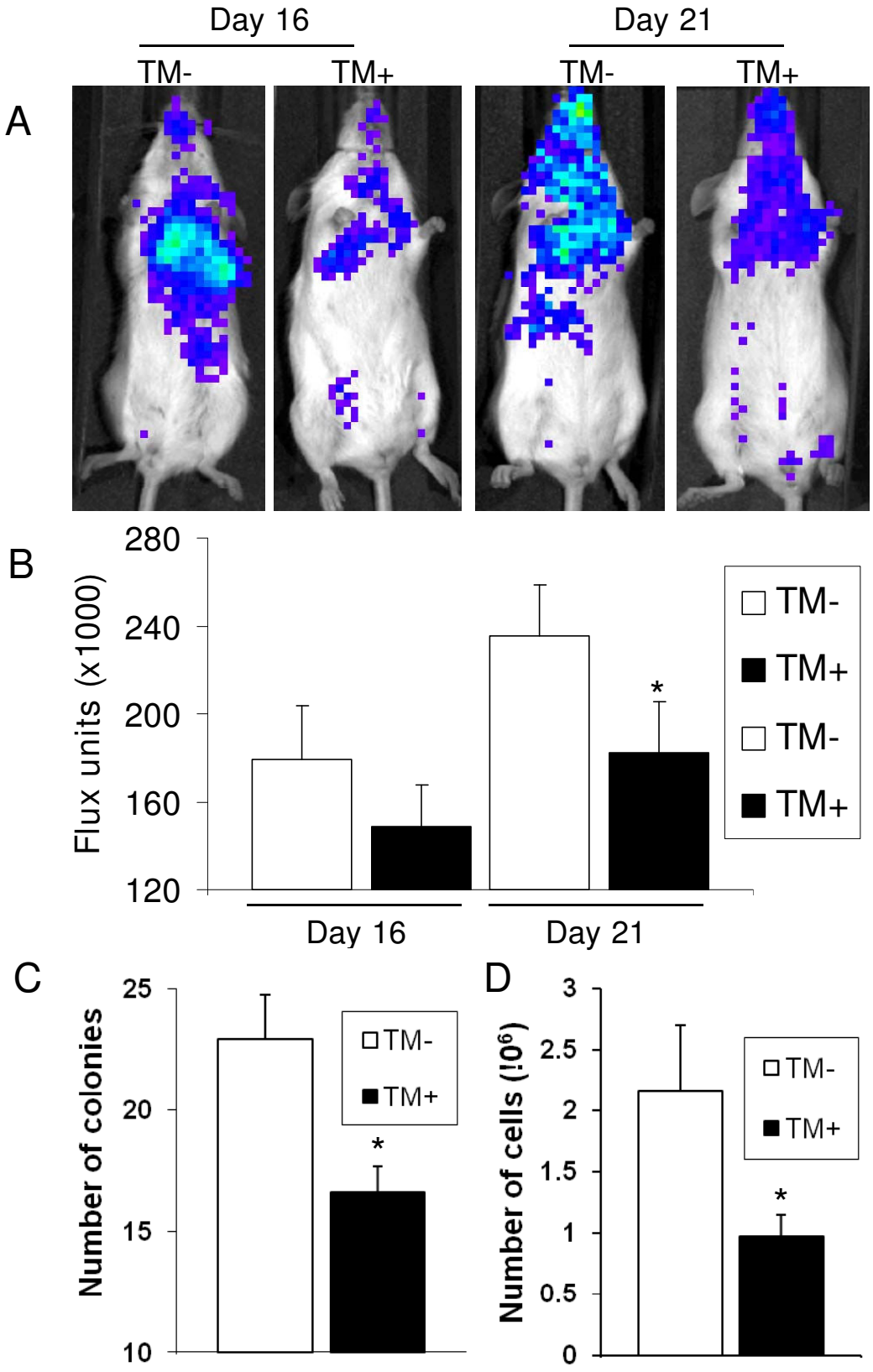
A
Day 16
Day 21
TM-
TM+
TM-
TM+
B
Flux units (x1000)
280
240
200
160
120
TM-
TM+
TM-
TM+
*
Day 16
Day 21
C
Number of colonies
25
20
15
10
TM-
TM+
*
D
Number of cells (!10⁶)
3
2.5
2
1.5
1
0.5
0
TM-
TM+
*

Figure 3

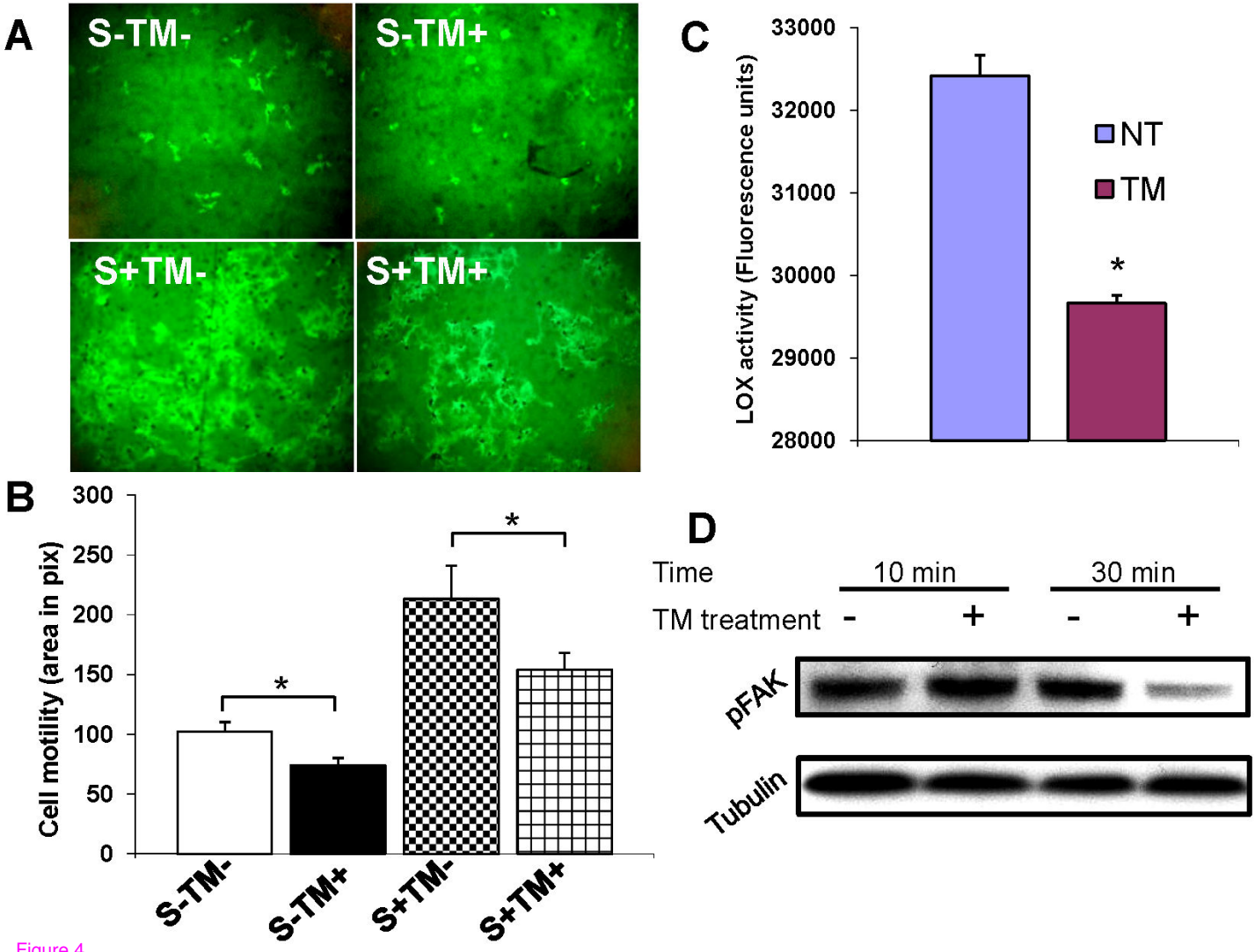
A
S-TM-
S-TM+
S+TM-
S+TM+
B
Cell motility (area in pix)
300
250
200
150
100
50
0
*
*
S-TM-
S-TM+
S+TM-
S+TM+
C
LOX activity (Fluorescence units)
33000
32000
31000
30000
29000
28000
NT
TM
*
D
Time
10 min
30 min
TM treatment
-
+
-
+
pFAK
Tubulin

Figure 4

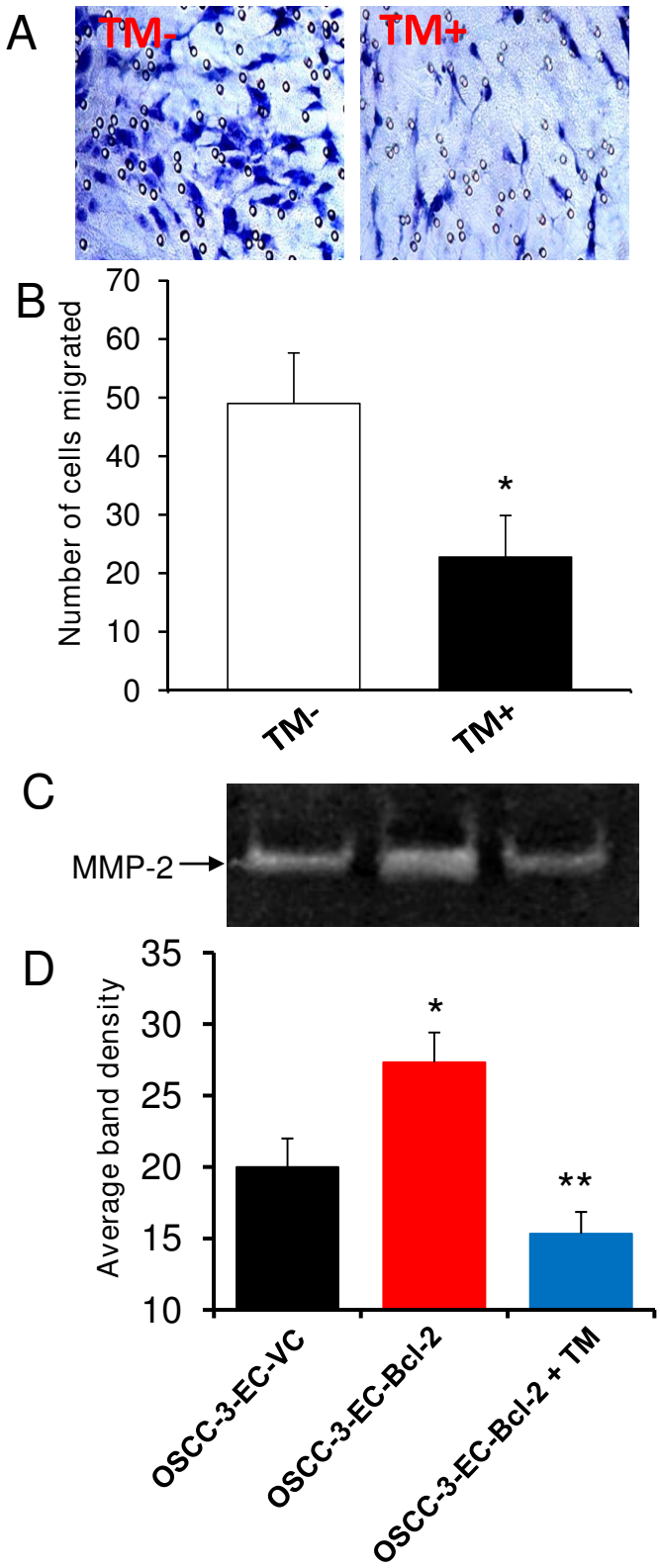
A
TM-
TM+
B
Number of cells migrated
70
60
50
40
30
20
10
0
*
TM-
TM+
C
MMP-2
D
Average band density
35
30
25
20
15
10
*
**
OSCC-3-EC-VC
OSCC-3-EC-Bcl-2
OSCC-3-EC-Bcl-2 + TM

Figure 5

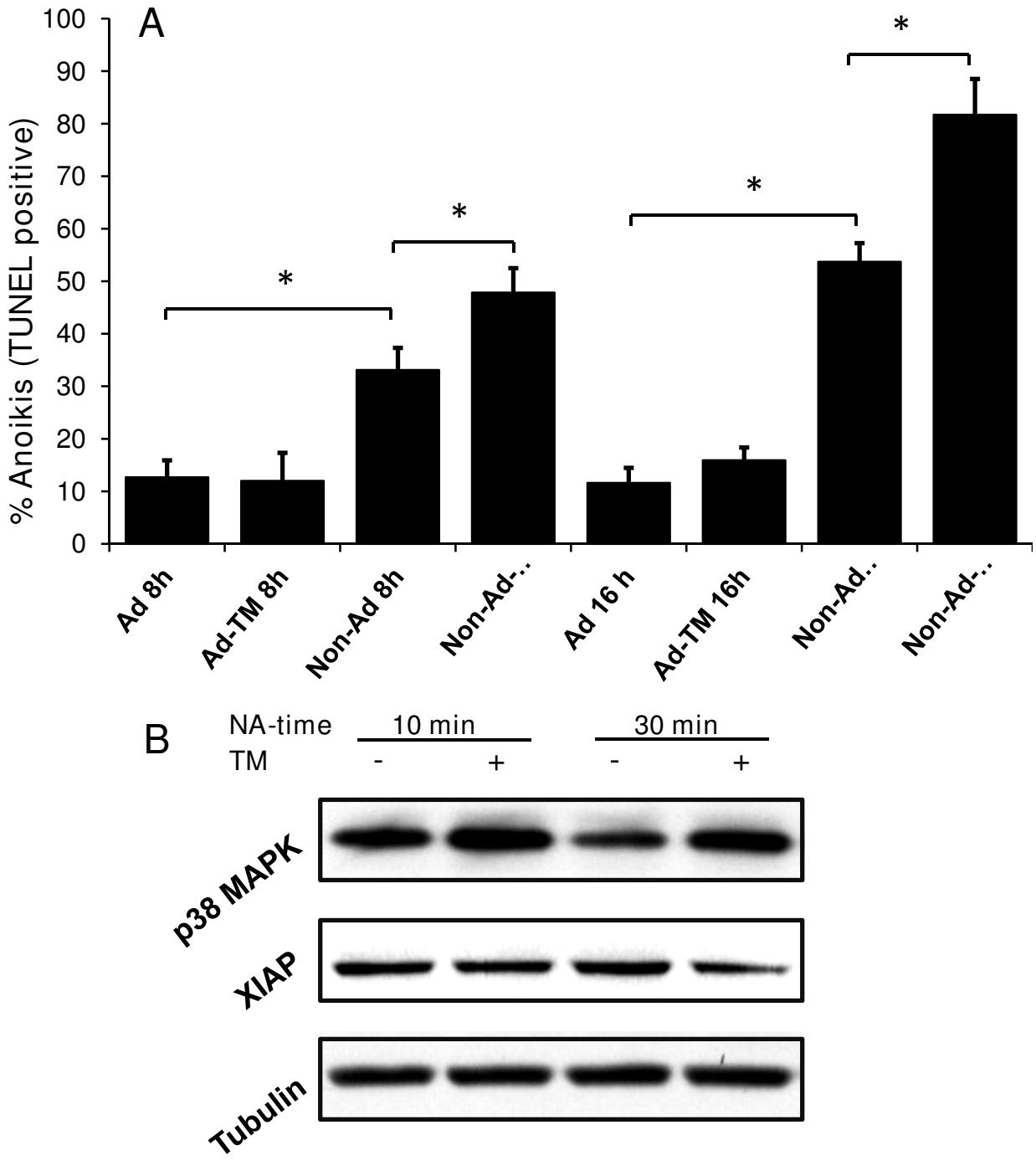
A
% Anoikis (TUNEL positive)
100
90
80
70
60
50
40
30
20
10
0
*
*
*
*
Ad 8h
Ad-TM 8h
Non-Ad 8h
Non-Ad-..
Ad 16 h
Ad-TM 16h
Non-Ad..
Non-Ad-..
B
NA-time
10 min
30 min
TM
-
+
-
+
p38 MAPK
XIAP
Tubulin

Figure 6